International Journal of Applied Mathematics

Volume 38 No. 9s, 2025

ISSN: 1311-1728 (printed version); ISSN: 1314-8060 (on-line version)

TRANSIENT STABILITY ASSESSMENT OF HYBRID AC–DC MICROGRID USING DISCRETE WAVELET TRANSFORM

[1] Sowmya Anand, [2] Dr.L.Sanjeev Kumar

[1]Research scholar, Department of Electrical and Electronics Engineering,

Sri Siddhartha Academy of Higher Education (SSAHE)

Tumkur , Karnataka, sowmy03@gmail.com

[2]Principal,Sri Siddhartha school of engineering

Tumkur, karnataka, sanjeev_ssit@yahoo.co.in

Corresponding Author: sowmy03@gmail.com

Abstract

This paper presents a comprehensive transient stability assessment of a hybrid AC–DC microgrid under diverse disturbances, including single- and multi-phase faults, source/load switching, and islanding conditions at varying battery states of charge (SoC). A Discrete Wavelet Transform (DWT) using the Daubechies-4 (DB4) mother wavelet is employed to decompose multi-domain signals—AC voltage, system frequency, and DC-link voltage—into approximation and detail coefficients. From these coefficients, statistical features such as energy, standard deviation, skewness, kurtosis, and entropy are extracted to quantify dynamic responses. Simulation results demonstrate that while the system exhibits rapid recovery from grid-side faults and switching events (voltage deviations limited to 0.74–0.99 pu, frequency restored within 0.25 s), islanding with insufficient SoC (≤20%) causes severe instability, characterized by voltage collapse (0.1 pu), frequency excursions (±0.25 Hz), and entropy escalation. The results confirm that DWT-based feature extraction provides early instability indicators with high sensitivity, highlighting the critical roles of inverter-based control and adequate SoC in ensuring stable islanded operation. The proposed framework serves as a diagnostic tool for real-time monitoring and adaptive control in hybrid microgrids.

Keywords—Hybrid AC–DC microgrid, transient stability, discrete wavelet transform, DB4 wavelet, islanding, power quality.

I. Introduction

Microgrids are central to future power systems, enabling integration of distributed renewable sources, improving resilience, and enhancing reliability [1], [2]. Among microgrid architectures, hybrid AC–DC systems offer improved efficiency and reduced conversion losses by directly supporting both AC and DC loads [3], [4]. However, hybrid AC–DC topologies also introduce dynamic coupling challenges that complicate transient stability analysis, particularly under faults, sudden switching, and islanding scenarios [5], [6].

Unlike large synchronous grids, microgrids are predominantly inverter-based and lack natural inertia, making them more vulnerable to frequency excursions and stability loss [7]. Grid-

Volume 38 No. 9s, 2025
ISSN: 1311-1728 (printed version); ISSN: 1314-8060 (on-line version)

forming control strategies, virtual inertia emulation, and adaptive droop mechanisms have been proposed to mitigate these challenges [8]–[10]. Yet, islanding at low SoC remains a critical vulnerability that requires further study.

Accurate detection and characterization of transient events is essential. Traditional Fourier-based methods are inadequate for analyzing non-stationary power system disturbances [11]. Discrete Wavelet Transform (DWT) has emerged as a powerful tool for transient analysis due to its ability to localize events in both time and frequency domains [12], [13]. Among wavelet families, the Daubechies-4 (DB4) wavelet is widely used in power system applications for its compact support and effectiveness in capturing both abrupt transitions and smooth trends [14], [15].

This paper applies DWT-based feature extraction to evaluate transient stability in a hybrid AC–DC microgrid under a comprehensive set of scenarios, including single- and multi-phase faults, wind/solar/load switching, and islanding at different battery SoC levels. The contribution lies in demonstrating how statistical features derived from DWT can provide early detection and quantification of instability, while highlighting the need for improved control and energy storage support during islanding.

II. Literature Review

The growing deployment of renewable resources and inverter-based systems has motivated extensive research into microgrid stability. This review is structured into key thematic areas.

A. Wavelet Transform Applications in Power Systems

The Discrete Wavelet Transform (DWT) has been widely applied for power quality disturbance detection, transient analysis, and fault classification. Compared to Fourier-based methods, DWT provides superior time-frequency localization for non-stationary signals [11], [12]. Mallat’s multi-resolution theory [13] and Daubechies’ compactly supported wavelets [14] form the mathematical foundation for wavelet-based decomposition. Several studies demonstrate DWT’s effectiveness in fault analysis [15], [16], islanding detection [17], [18], and transient stability assessment [19]. The Daubechies-4 (DB4) wavelet, in particular, is effective in capturing sharp transients and smooth variations, making it a preferred choice for electrical signal analysis [20], [21].

B. Statistical Features from DWT

Beyond waveform decomposition, statistical features extracted from DWT coefficients provide quantitative indicators of system dynamics. Energy approximation and standard deviation are widely used to assess system stability margins [22]. Higher-order moments such as kurtosis and skewness are effective in distinguishing sharp transient spikes from gradual drifts [23], [24]. Entropy has been used to quantify randomness and identify instability under islanding conditions [25], [26]. These features, when combined, enable robust stability characterization even under noisy operating conditions.

C. Hybrid Approaches: DWT with AI/ML

ISSN: 1311-1728 (printed version); ISSN: 1314-8060 (on-line version)

Recent research integrates DWT with artificial intelligence and machine learning classifiers such as artificial neural networks (ANN), support vector machines (SVM), and ensemble learners for improved classification accuracy [27], [28]. Such hybrid approaches enhance fault detection [29], power quality disturbance classification [30], and islanding identification [31]. However, many of these studies are limited to either fault or PQ disturbances, without holistic stability analysis across multiple disturbance types.

D. Hybrid AC–DC Microgrids

Hybrid AC–DC architectures have emerged to simultaneously support AC and DC loads while reducing conversion losses [32], [33]. However, the interlinking converter dynamics introduce complex interactions that can compromise transient stability [34], [35]. Several works have investigated fault ride-through [36], droop-based power sharing [37], and converter stability under disturbances [38]. Yet, few studies have comprehensively evaluated hybrid AC–DC microgrids under combined disturbances such as faults, switching events, and islanding.

E. Inverter Control and Energy Storage Systems

Grid-forming and grid-following inverters play a critical role in stabilizing microgrids [39], [40]. Virtual synchronous generator (VSG) techniques emulate inertia to enhance stability [41], while adaptive droop controls dynamically adjust power sharing to improve robustness [42], [43]. Energy storage systems (ESS), particularly batteries and supercapacitors, are vital for smoothing fluctuations [44]. Hybrid ESS configurations further improve voltage/frequency regulation and fault ride-through [45].

F. Validation and Experimental Studies

Hardware-in-the-loop (HIL) frameworks are increasingly used for validating microgrid controllers and stability studies [46], [47]. Such experimental validation ensures that wavelet-based monitoring and ESS control strategies can be translated into practical implementations.

While wavelet-based methods have been extensively used for PQ and fault analysis, limited studies have applied DWT-based statistical features to comprehensively evaluate hybrid AC–DC microgrid stability under diverse disturbances. Furthermore, the role of battery state of charge (SoC) in islanding stability has not been quantitatively studied with wavelet-based feature extraction.

This paper addresses these gaps by:

1. Analyzing faults, source/load switching, and islanding events together in a hybrid AC–DC microgrid.
2. Monitoring multi-domain signals (AC voltage, AC frequency, and DC link voltage).
3. Employing DWT-based statistical feature extraction (energy, standard deviation, kurtosis, skewness, entropy) for quantitative stability assessment.
4. Demonstrating the critical role of battery SoC in determining islanding stability.
5.

International Journal of Applied Mathematics
Volume 38 No. 9s, 2025
ISSN: 1311-1728 (printed version); ISSN: 1314-8060 (on-line version)

III. Proposed Methodology

The proposed methodology for transient stability assessment of the hybrid AC–DC microgrid is illustrated in Fig. 1.

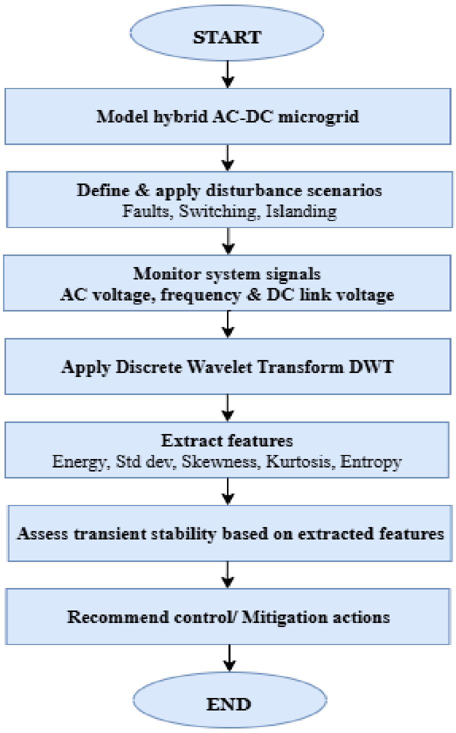

Figure.1: Proposed Methodology

The framework consists of four key stages:

1. **System Modeling:** A hybrid AC–DC microgrid is developed comprising solar PV, wind turbine, battery storage, AC loads, and DC loads as in fig.2. The microgrid operates in both grid-connected and islanded modes.

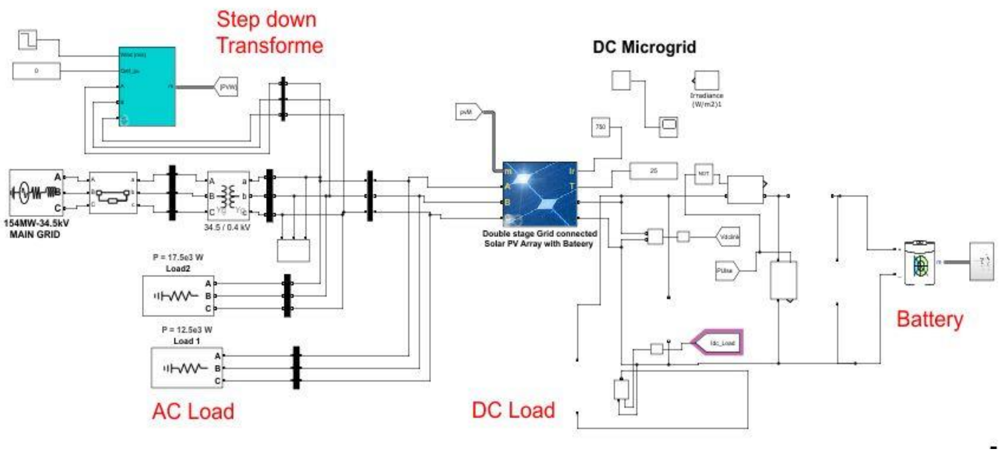

Figure 2: Test System

International Journal of Applied Mathematics

Volume 38 No. 9s, 2025

ISSN: 1311-1728 (printed version); ISSN: 1314-8060 (on-line version)

2. **Disturbance Scenarios:** Different disturbances are applied, including single- and multi-phase faults (LG, LLG, LLLG), source/load switching, and islanding at various battery SoC levels (80% and 20%).

3. **DWT-Based Signal Decomposition:** Multi-domain signals (AC bus voltage, frequency, and DC-link voltage) are analysed using the Discrete Wavelet Transform (DWT) with Daubechies-4 (DB4) wavelet to capture both slow variations and fast transients as shown in Fig.3. DWT with DB4 wavelet is applied to voltage, frequency, and DC link signals. Approximation coefficients represent slow dynamics, while detail coefficients capture fast transients.

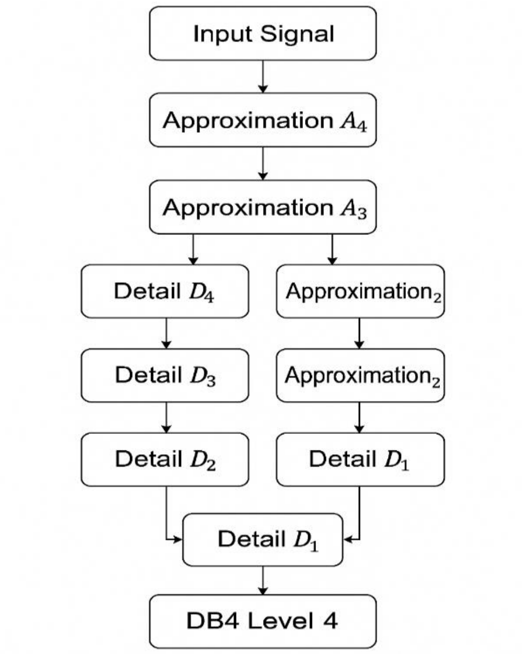

Figure 3: DWT working

To capture both the fast transients and the slow-varying dynamics of the hybrid AC–DC microgrid signals (AC bus voltage vac(t), system frequency f(t), and DC link voltage vdc(t), the **Discrete Wavelet Transform (DWT)** with Daubechies-4 (db4) mother wavelet is employed.

The one-dimensional DWT decomposes a signal x(t) into **approximation** (Aj) and **detail** (Dj) coefficients at successive scales j:

$$A_j[k] = \sum_n x[n]\phi_{j,k}[n] \quad (1)$$

$$D_j[k] = \sum_n x[n]\varphi_{j,k}[n] \quad (2)$$

$\phi_{j,k}[n] = 2^{-j/2}\phi(2^{-j}n - k) is\ the\ scaling\ function$

$\varphi_{j,k}[n] = 2^{-j/2}\varphi(2^{-j}n - k) is\ the\ wavelet\ function$

$j\ is\ the\ decomposistion\ level\ and\ k\ the\ translation\ index$

Low-pass and high-pass quadrature mirror filters h[n] and g[n] implement the above via a multiresolution filter bank:

Volume 38 No. 9s, 2025
ISSN: 1311-1728 (printed version); ISSN: 1314-8060 (on-line version)

$$A_j[k] = \sum_n h[n-2k]A_{J-1}[n] \quad (3)$$

$$D_j[k] = \sum_n g[n-2k]A_{j-1}[n] \quad (4)$$

Approximation coefficients A_j capture the slow (low-frequency) behaviour, while detail coefficients D_j isolate the high-frequency transients produced by faults, switching, or islanding.

4. **Feature Extraction and Stability Assessment:** Statistical features such as energy, standard deviation, skewness, kurtosis, and entropy are extracted from the DWT coefficients to quantify system response and identify instability indicators.

From the DWT coefficients, statistical feature is computed to quantify the severity of each disturbance:

1. Energy of approximation coefficients

$$E_{approx} = \sum_k \left|A_j[k]\right|^2 \quad (5)$$

A drop in energy signals a loss of steady –state power or voltage magnitude.

2. Standard deviation

$$\sigma = \sqrt{\frac{1}{N}\sum_k (A_j[k]-\mu)^2} \quad (6)$$

$$\mu = \frac{1}{N}\sum_k A_j[k] \quad (7)$$

Larger σ reflects stronger oscillations and instability.

3. Skewness

$$Skew = \frac{1}{N}\sum_k \left(\frac{A_j[k]-\mu}{\sigma}\right)^3 \quad (8)$$

Indicates asymmetry of the transient distribution.

4. Kurtosis

$$Kurt = \frac{1}{N}\sum_k \left(\frac{A_j[k]-\mu}{\sigma}\right)^4 \quad (9)$$

High kurtosis points to sharp spikes such as those created by faults.

5. Shannon entropy

$$H = -\sum_k p_k \log p_k \quad (10)$$

$$p_k = \frac{|A_j[k]|^2}{\sum_m |A_j[k]|^2} \quad (11)$$

Entropy measures the randomness or disorder in the signal; a rise indicates growing instability.

These metrics—calculated for voltage, frequency, and DC link voltage—provide quantitative indicators of transient stability. In particular, a simultaneous drop in E_{approx} and rise in σ and H reliably flags unstable islanding when the battery state of charge (SoC) is low.

Received: August 08, 2025

International Journal of Applied Mathematics
Volume 38 No. 9s, 2025
ISSN: 1311-1728 (printed version); ISSN: 1314-8060 (on-line version)

IV. Results and Discussion

A. Faults

Case 1: Single Line to Ground Fault (L-G) near the step-down transformer

A single LG fault near the step-down transformer causes a mild voltage sag to 0.992 p.u. (Fig. 4) with complete restoration within 0.2 seconds. Frequency at all monitored buses dips slightly to 49.8 Hz (Fig. 5), before rapidly settling to nominal. The DC link voltage (Fig. 6) is effectively isolated from AC-side transients, maintaining robust stability at 470 V. Discrete Wavelet Transform (DWT) decomposition exposes a clear dip in approximation coefficients and oscillatory spikes in the detail coefficients (Figs. 7–9), identifying momentary energy dissipation and harmonic activity at the fault instant. These results confirm the effectiveness of inverter-based controls in containing single-phase faults and ensuring rapid system recovery.

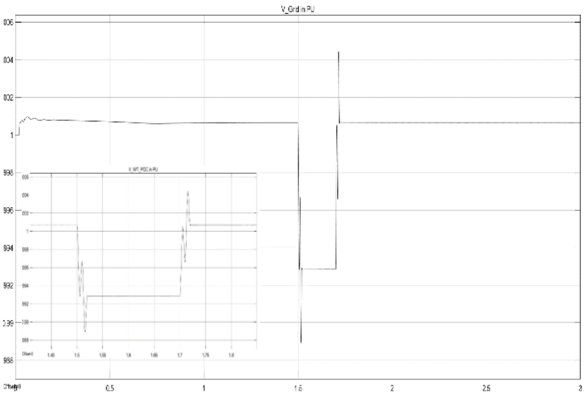

Figure 4: Grid voltage in PU-Case1

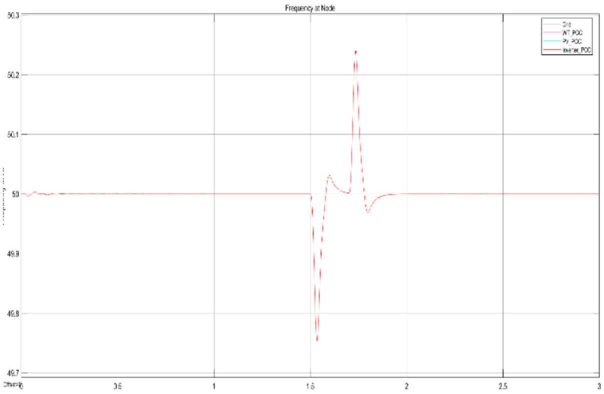

Figure 5: Frequency at various Buses- Case 1

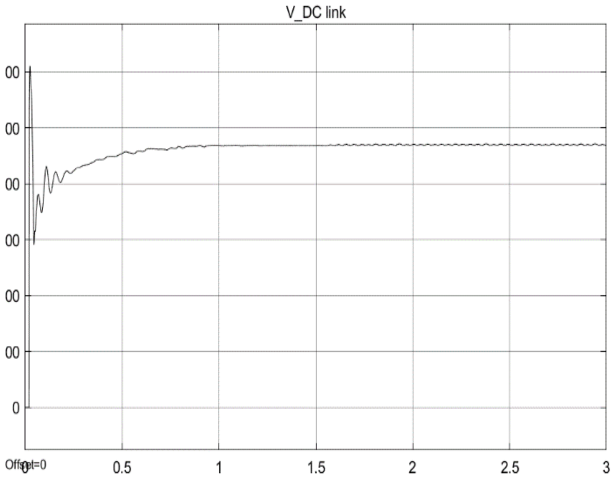

Figure 6: DC Link Voltage-Case 1

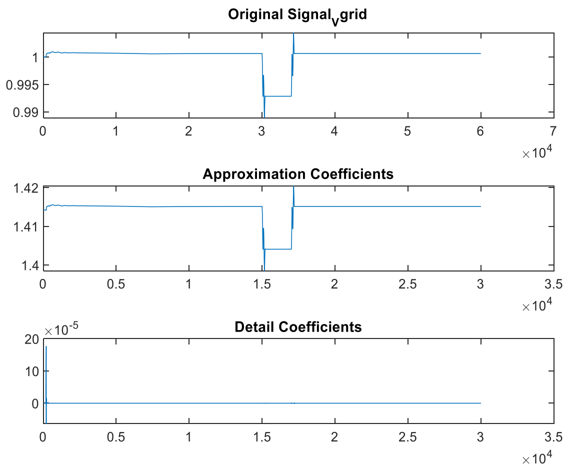

Figure 7: Decomposition of Grid voltage- Case 1

International Journal of Applied Mathematics
Volume 38 No. 9s, 2025
ISSN: 1311-1728 (printed version); ISSN: 1314-8060 (on-line version)

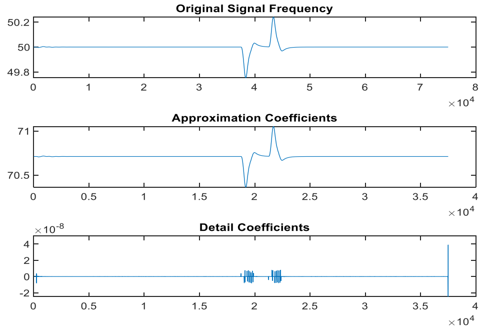

Figure 8: Decomposition of Frequency Voltage -Case 1

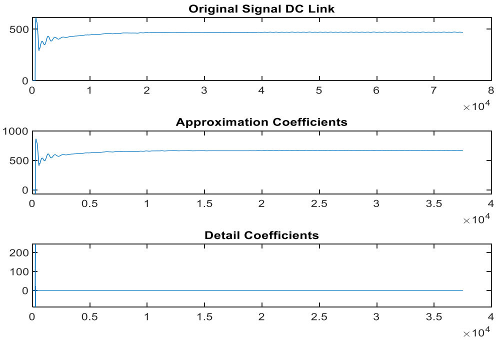

Figure 9: Decomposition of DC Link

Case 2: LLG Fault at same location as in case 1

The LLG fault leads to a deeper voltage sag (to 0.74 p.u., Fig. 10) and a larger frequency excursion (minimum of 49.7 Hz, Fig. 11), though recovery time remains under 0.25 seconds. DC link voltage (Fig. 12) shows high resilience, preserving voltage levels. DWT analysis (Figs. 13–15) highlights stronger, more sustained oscillations in the detail coefficients, indicative of increased system stress under multiphase disturbance. The ability of the inverter to maintain DC voltage despite increased AC side disturbance is validated.

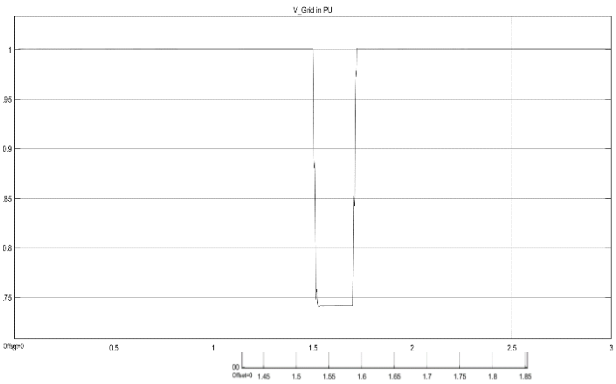

Figure 10: Grid voltage in PU-Case 2

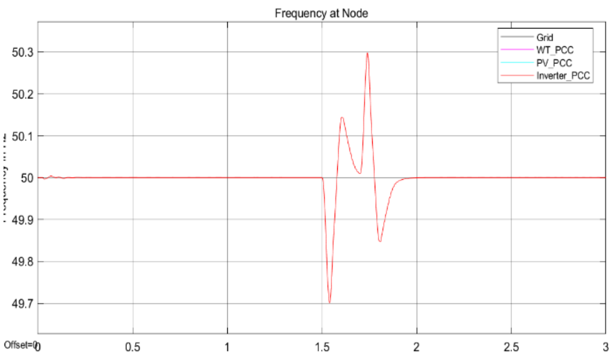

Figure 11: Frequency at various Buses-Case 2

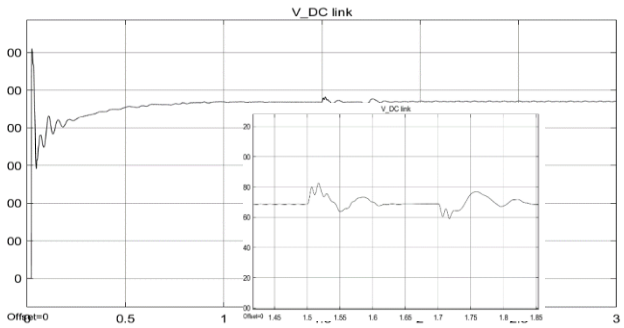

Figure 12: DC Link Voltage –Case2

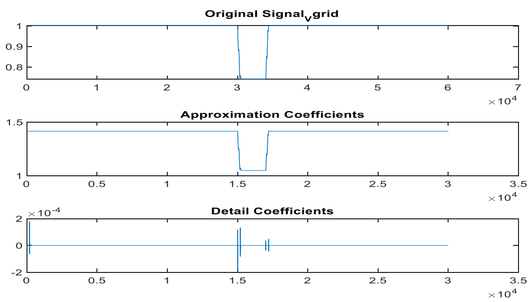

Figure 13: Decomposition of Grid Voltage

International Journal of Applied Mathematics

Volume 38 No. 9s, 2025

ISSN: 1311-1728 (printed version); ISSN: 1314-8060 (on-line version)

using Db4-Case 2

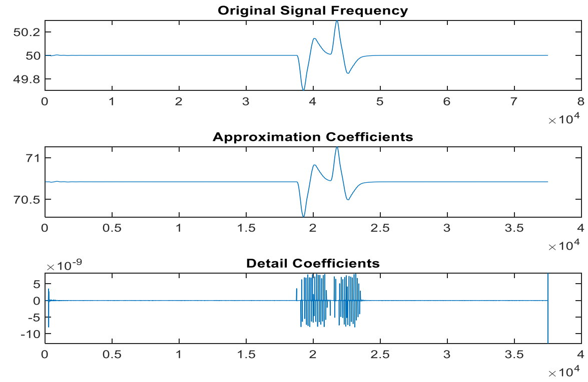

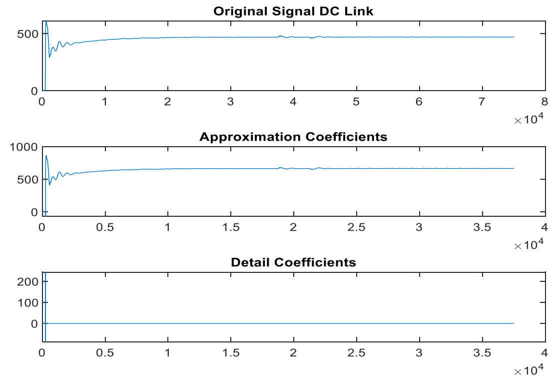

Figure 14: Decomposition of Frequency using **Figure 15:** Decomposition of DC Link Voltage

Db4-Case 2

Case 3: LLLG fault:

With LLLG faults, voltage collapses sharply to 0.58 p.u. (Fig. 16), with frequency dipping to 49.7 Hz (Fig. 17) and requiring up to 0.3 seconds to recover. DC link voltage (Fig. 18) remains stable, demonstrating strong decoupling by interlinking converters. DWT results (Figs. 19–21) show a high density of oscillatory detail coefficients, typical of severe system-wide faults. These trends confirm that as fault severity increases, AC variables (voltage, frequency) are more affected, while the DC subsystem remains comparatively resilient.

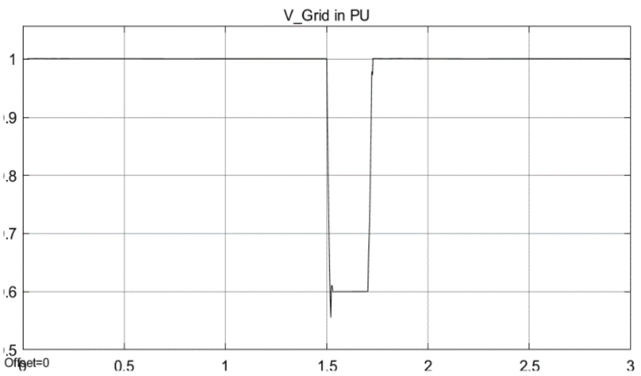

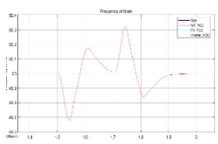

Received: August 08, 2025

International Journal of Applied Mathematics
Volume 38 No. 9s, 2025
ISSN: 1311-1728 (printed version); ISSN: 1314-8060 (on-line version)

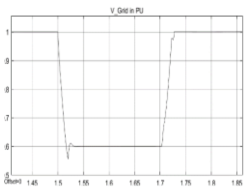

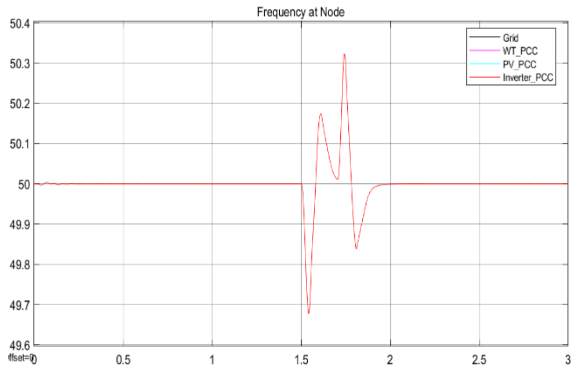

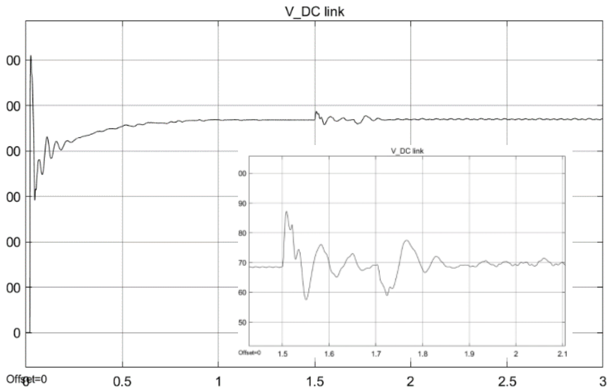

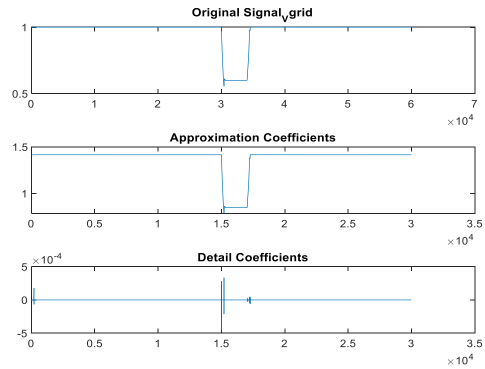

Figure 16: Grid voltage in PU-Case 3 **Figure 17:** Frequency at various Buses-Case 3

ase 3 **Figure 19:** Decomposition of Grid voltage using Db4-Case 3

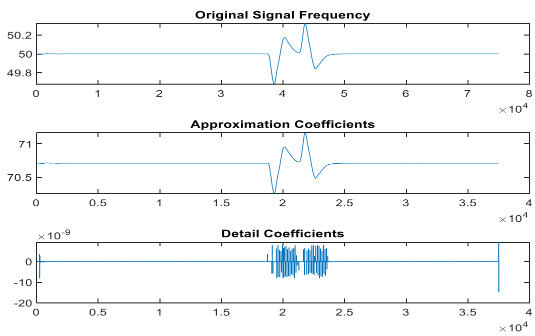

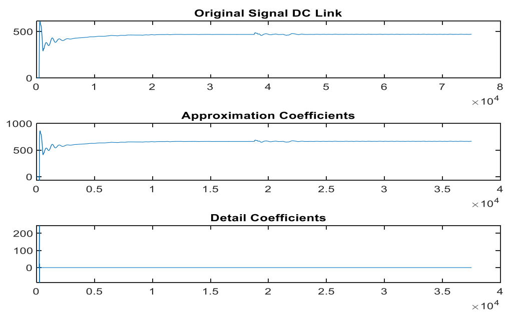

Figure 20: Decomposition of Frequency using **Figure 21:** Decomposition of DC Link

Voltage using Db4-Case 3

B. Switching Events

Case 4: WT switching at 1.5 sec

Switching the wind turbine at 1.5 s produces a slight voltage sag to 0.995 p.u. (Fig. 22) with frequency deviation of only 0.05 Hz (Fig. 23). The DC link (Fig. 24) remains unaffected. DWT (Figs. 25–26) locates oscillatory spikes exactly at the switching instant, confirming temporal

Received: August 08, 2025

International Journal of Applied Mathematics
Volume 38 No. 9s, 2025
ISSN: 1311-1728 (printed version); ISSN: 1314-8060 (on-line version)

precision of feature extraction and confirming the system's prompt stabilization after renewable source switching.

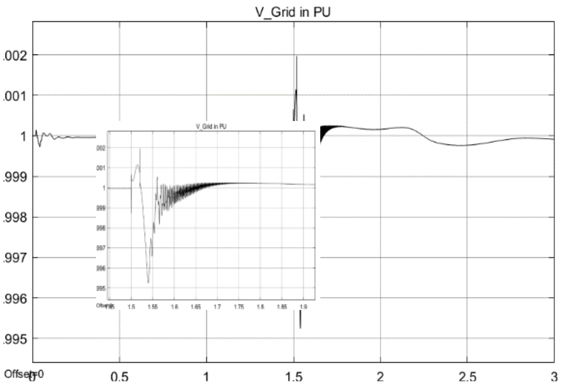

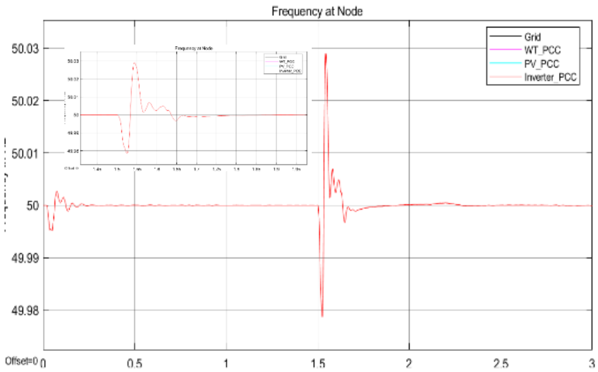

Figure 22: Grid voltage in PU-Case 4 **Figure 23:** Frequency at various Buses-

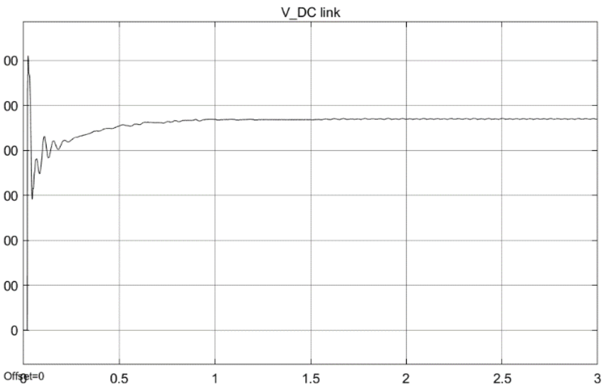

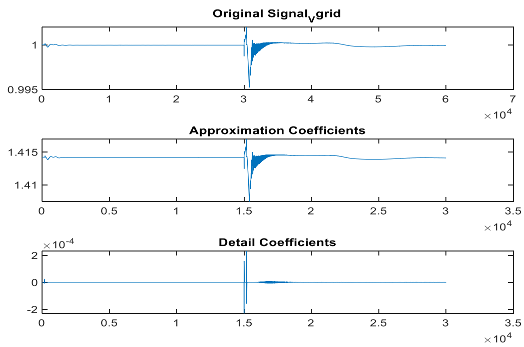

Case 4

Figure 24: DC Link Voltage-Case 4 **Figure 25:** Decomposition of Grid Voltage using Db4-Case 4

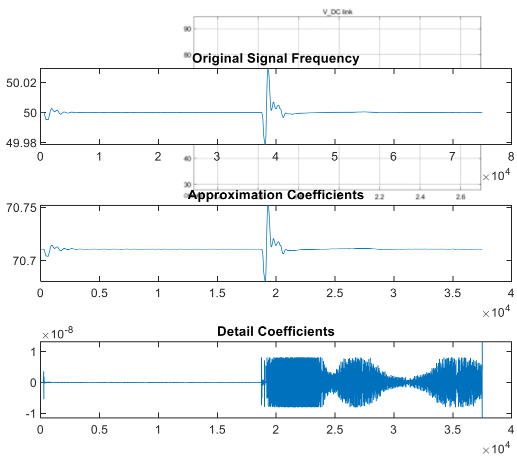

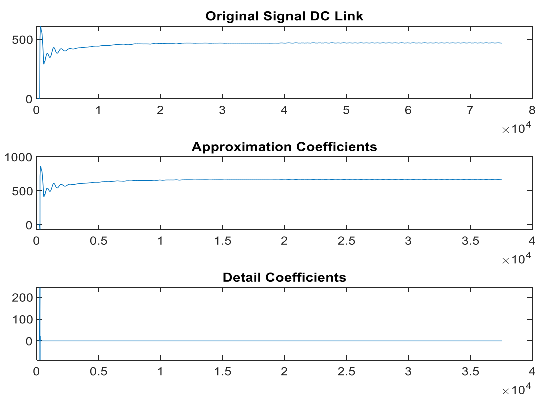

Figure 26: Decomposition of Frequency using **Figure 27:** Decomposition of DC Link Voltage

International Journal of Applied Mathematics
Volume 38 No. 9s, 2025
ISSN: 1311-1728 (printed version); ISSN: 1314-8060 (on-line version)

using Db4-Case 4

Case 5: Switching down of Solar PV at 1.5 sec

Removal of a solar PV unit is nearly imperceptible in terms of grid voltage (1.0 p.u., Fig. 27), and both frequency and DC link voltage (Figs. 28–29) are undisturbed. DWT (Figs. 30–32) registers only brief, minor transients, reflecting balanced source/load flows and advanced DC bus management.

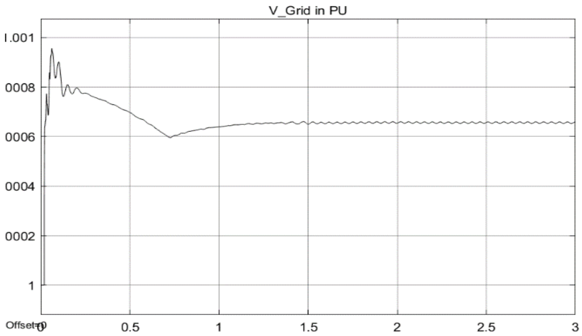

Figure 27: Grid voltage in PU-Case 5

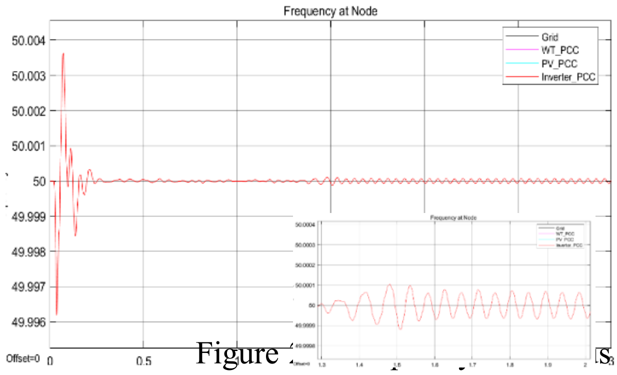

Figure

Buses-Case 5

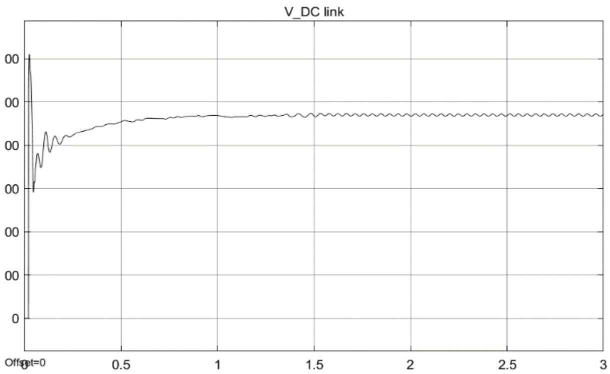

Figure 29: DC Link Voltage-Case

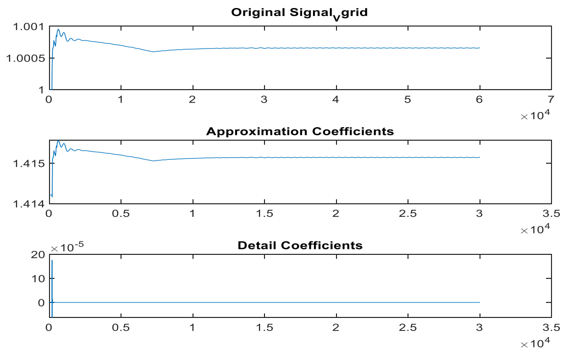

Figure 30: Decomposition of Grid Voltage using Db4-Case 5

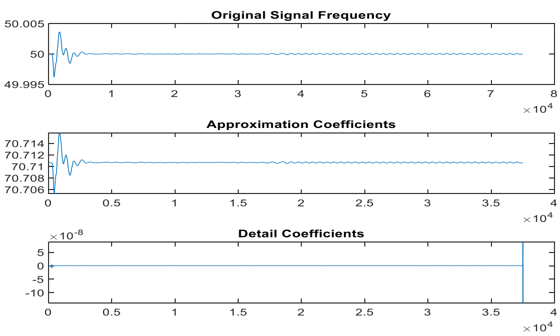

Figure 31: Decomposition of Frequency using

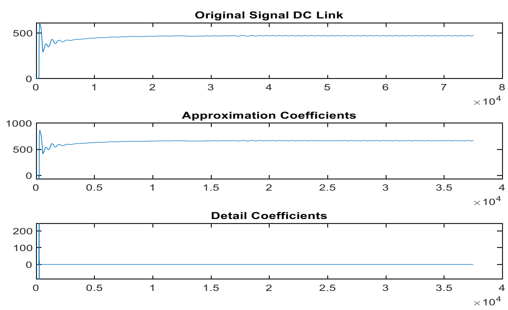

Figure 32: Decomposition of DC Link Voltage

Received: August 08, 2025

Volume 38 No. 9s, 2025

ISSN: 1311-1728 (printed version); ISSN: 1314-8060 (on-line version)

using Db4-Case 5

Case 6: Switching of 100kW load at 1.5Sec

Load switching results in a negligible voltage change (0.001 p.u., Fig. 33) and minimal frequency deviation (0.006 Hz, Fig. 34). The DC bus remains unwavering (Fig. 35). DWT figures (Figs. 36–38) confirm that oscillations are highly localized, underlining the microgrid's robust handling of routine load changes.

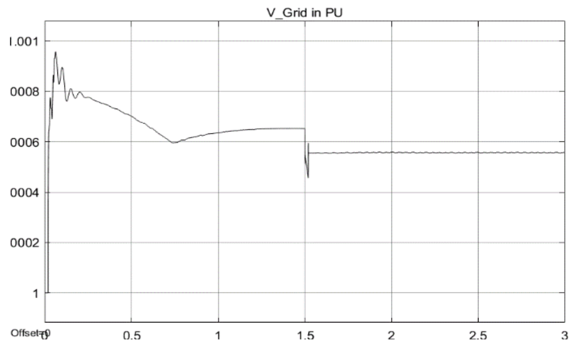

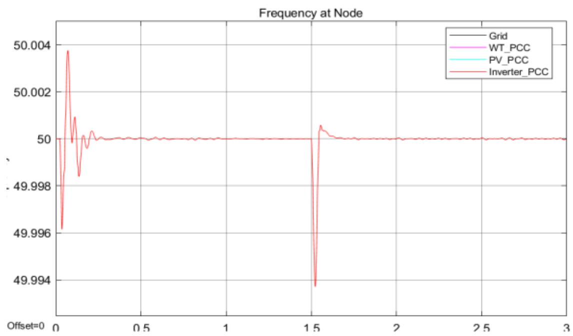

Figure 33: Grid voltage in PU-Case 6 **Figure 34:** Frequency at various Buses-Case 6

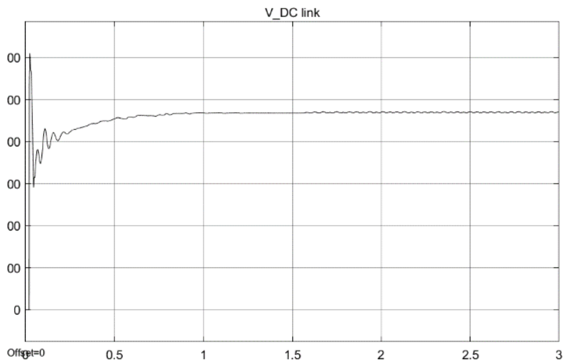

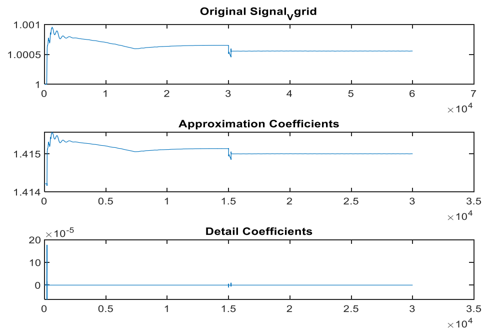

Figure 35: DC Link Voltage-Case 6 **Figure 36:** Decomposition of Grid Voltage

using Db4-Case 6

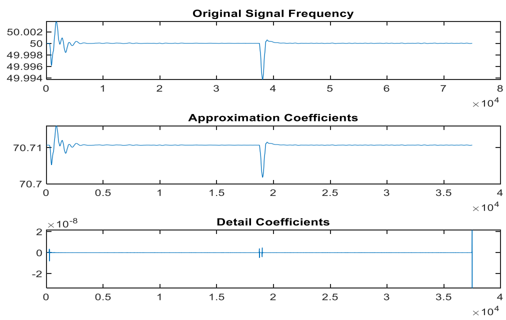

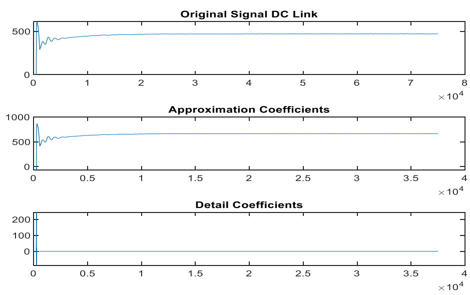

Figure 37: Decomposition of Frequency using **Figure 38:** Decomposition of DC Link Voltage

Volume 38 No. 9s, 2025
ISSN: 1311-1728 (printed version); ISSN: 1314-8060 (on-line version)

using Db4-Case 6

C. Islanding Scenarios

Case 7: Islanding at 1.5 sec with 80% SoC

When islanding occurs with battery at 80% SoC, the system shows marked vulnerability: voltage collapses to 0.15 p.u. (Fig. 39), and frequency exhibits large swings (49.9–50.6 Hz, Fig. 40). DC link voltage destabilizes (Fig. 41). DWT decompositions (Figs. 42–44) indicate loss of coherent approximation trends and persistent oscillations in detail coefficients, signaling a deviation from normal operation with limited energy support.

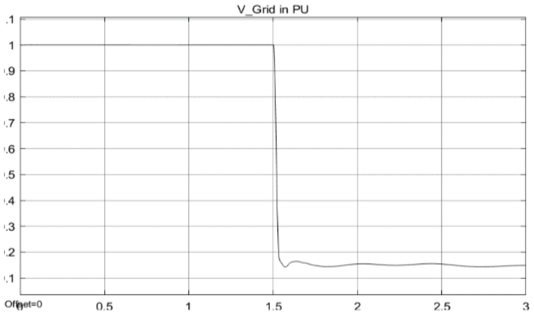

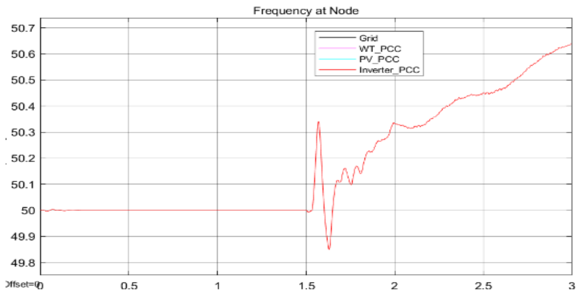

Figure 39: Grid voltage in PU-Case 7 **Figure 40:** Frequency at various Buses-

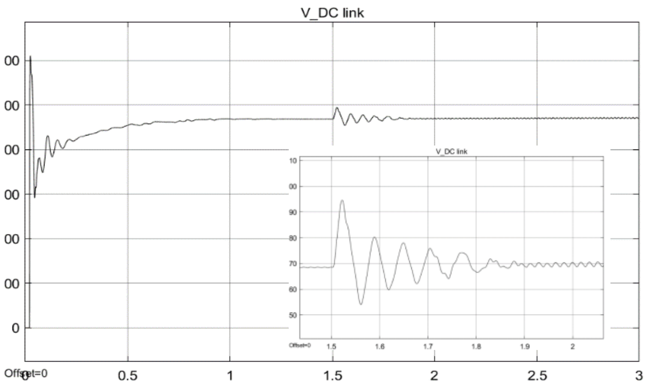

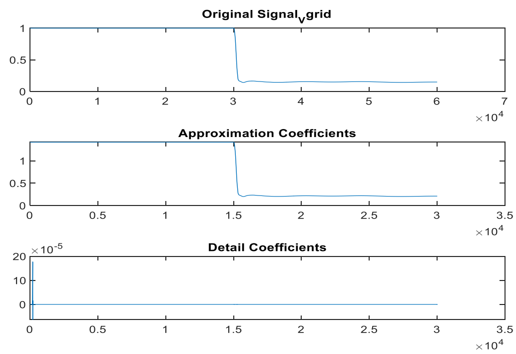

Case 7

Figure 41: DC Link Voltage-Case 7 **Figure 42:** Decomposition of Grid Voltage using

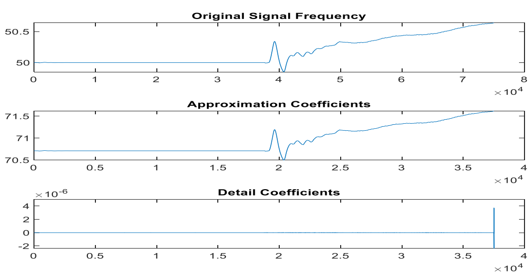

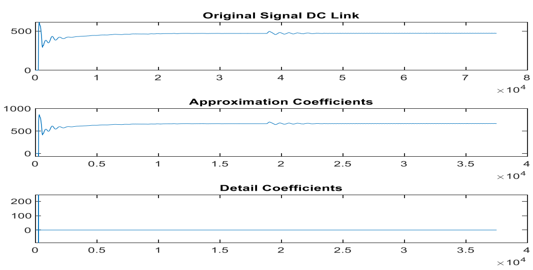

Db4-Case 7

Figure 43: Decomposition of Frequency using **Figure 44:** Decomposition of DC Link Voltage

International Journal of Applied Mathematics
Volume 38 No. 9s, 2025
ISSN: 1311-1728 (printed version); ISSN: 1314-8060 (on-line version)

using Db4-Case 7

Case 8: Islanding with SoC 25%

For critically low SoC (20–25%), voltage plunges to 0.1 p.u. (Fig. 45), frequency falls to 49.75 Hz with extreme oscillatory activity (Fig. 46), and DC link regulation fails (Fig. 47). DWT

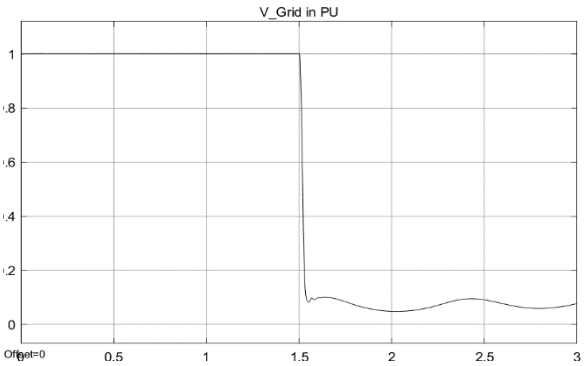

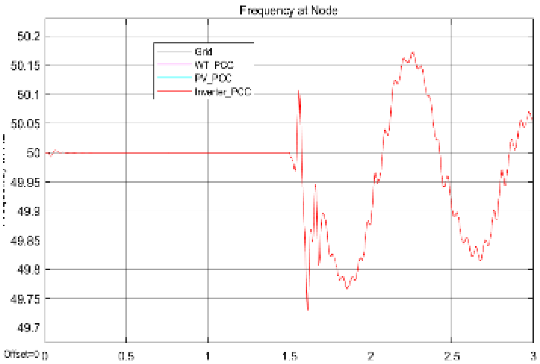

results (Figs. 48–50) show sustained, high-frequency oscillations throughout the islanded interval. The results establish that poor storage conditions severely undermine islanded stability, overriding the resilience seen in other disturbance cases.

Figure 45: Grid voltage in PU-Case 8 **Figure 46:** Frequency at various Buses-Case 8

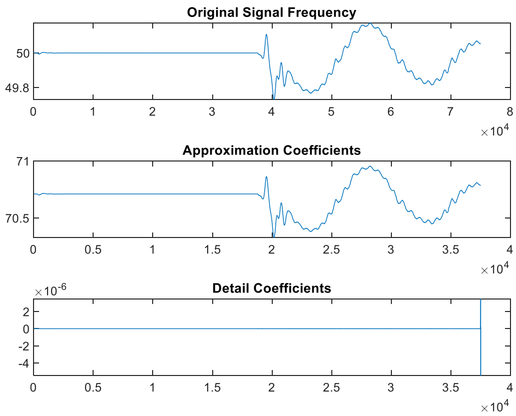

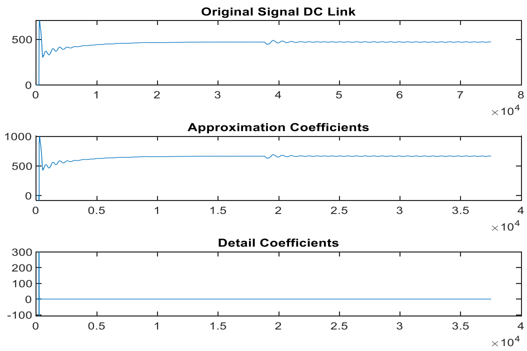

Figure 47: DC Link Voltage-Case 8 **Figure 48:** Decomposition of Grid Voltage using Db4-Case 8

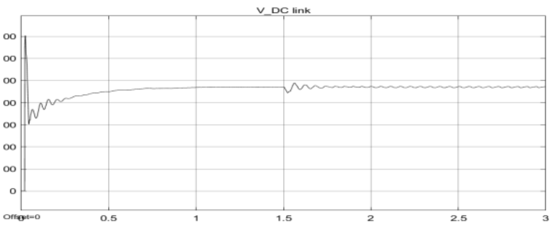

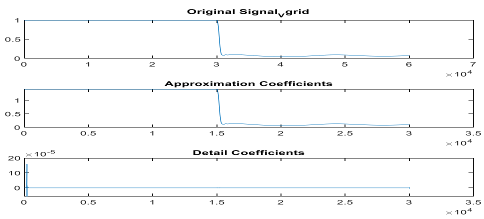

Figure 49: Decomposition of Frequency using **Figure 50:** Decomposition of DC Link Voltage

using Db4-Case 8

Received: August 08, 2025

International Journal of Applied Mathematics

Volume 38 No. 9s, 2025

ISSN: 1311-1728 (printed version); ISSN: 1314-8060 (on-line version)

Table 1: Voltage and Frequency Response Characteristics Under Different Fault, Switching, and Islanding Conditions

Condition	Voltage (Steady-State)	Voltage (Transient)	Frequency (Steady-State)	Frequency (Transient)	Settling Time (Sec)
Base Case	1.0 p.u.	1.0 p.u.	50 Hz	50 Hz	-
LG Fault	1.001 p.u.	0.992 p.u.	50 Hz	49.8 Hz	~0.03s/0.2s
LLG Fault	1 p.u.	0.74 p.u.	50 Hz	49.7 Hz	~0.03s/0.2s
LLLG Fault	1 p.u.	0.58 p.u.	50 Hz	49.7 Hz	~0.03s/0.2s
Load Switching	1.0 p.u.	1 p.u.	50 Hz	49.994 Hz	-
Solar Switching	1.0 p.u.	1 p.u.	50 Hz	50 Hz	-
WT Switching	1 p.u.	0.995 p.u.	50 Hz	49.98 Hz	~0.4s/0.15s
Islanding (80% SoC)	1 p.u.	0.15 p.u.	50 Hz	50.6 Hz	~Unstable
Islanding (20% SoC)	1 p.u.	0.1 p.u.	50 Hz	49.75 Hz	Unstable

D. Feature Insights

Table 2: Features of Grid Voltage extracted using DWT

features	Base case	LG Fault	LLG fault	LLLG fault	Load switching	Solar Switching	WT Switching	Islanding with 80% SoC	Islanding with 20% SoC
Energy_approx	60087	60025	58267	57404	60081	60087	60001	31040	30514
std_approx	0.000107	0.002774	0.089922	0.141546	0.000135	0.000106	0.000482	0.59935283	0.654729462

ISSN: 1311-1728 (printed version); ISSN: 1314-8060 (on-line version)

skewness_detail	136	136	10.16497	-13.9624	134.6701	136.2986	0.155781	136.301326	136.2377605
kurtosis_approx	42.81329	13.35183	13.10225	12.61636	14.18238	44.21345	89.87233	1.00539758	1.007687326
entropy_approx	-41729	-41624	-39118	-38287	-41719	-41729	-41583	-18901.	-20241.

Energy approximation values fall by nearly 50% during islanding, with standard deviation peaking (0.65 for islanding, vs. 0.14 for severe faults), clearly identifying the system's stressed profile. Kurtosis and skewness are sensitive to rapid event transitions, and entropy increases substantially as instability grows during low SoC islanding.

Table 3: Features of Grid Frequency extracted using DWT

feature_names	Base case	LG Fault	LLG Fault	LLLG Fault	**Load switching**	**Solar Switching**	**WT Switching**	**Islanding with 80%SoC**	**Islanding with 20% SoC**
energy_approx	18752000 3	18751954 7	18751641 6	18752111 6	187519706	187520001	187520699	188863293	187320133
std_approx	0.00054	0.04479	0.06738	0.07425	0.00086	0.00053	0.00376	0.30946	0.12478
skewness_detail	-69.70	31.01	-1.24	-1.82	-63.84	-72.63	0.02	73.14	-73.12
kurtosis_approx	62.11	40.46	21.96	20.93	54.62	60.93	68.99	1.91	3.19
entropy_approx	-1597144099	-1597139902	-1597110296	-1597155099	-1597141270	-1597144075	-1597150722	-1609940434	-1595243170

Entropy and standard deviation sharply increase for low SoC islanding, with kurtosis dropping, thereby signaling a loss of dynamic regularity. DWT-based feature extraction reveals that oscillatory trends in the detail coefficients are robust predictors of system health and fault type.

Volume 38 No. 9s, 2025
ISSN: 1311-1728 (printed version); ISSN: 1314-8060 (on-line version)

Table 4: Feature extraction of DC Link voltage using DWT

Condition	Energy Approx	Std Approx	Kurtosis	Entropy Approx	Impact on DC Voltage
Base Case	1.59E+10	62.35	79.94	-2.06E+11	Stable DC Voltage
LG Fault	1.59E+10	62.34	79.94	-2.06E+11	No Significant Impact
LLG Fault	1.59E+10	62.37	79.79	-2.06E+11	No Significant Impact
LLLG Fault	1.59E+10	62.40	79.65	-2.06E+11	Minimal DC Disturbance
Load Switching	1.59E+10	62.35	79.93	-2.06E+11	Well-Managed Variations
Solar Switching	1.59E+10	62.38	79.71	-2.06E+11	No Major Effect
WT Switching	1.59E+10	62.34	79.94	-2.06E+11	Stable Response
Islanding (80%)	1.59E+10	62.53	79.16	-2.06E+11	Slight Variations, Stable
Islanding (20%)	1.58E+10	**66.02**	**64.42**	**-2.05E+11**	**Severe Instability**

In all fault and switching cases, DC link energy and standard deviation remain stable, whereas during islanding, especially at low SoC, energy drops sharply, standard deviation rises, and kurtosis/entropy shift, reflecting loss of DC-side regulation

E. Key Observations

Table 5: Impact of Different condition on DC side

Condition	Impact on DC Link Voltage	Reason
LG, LLG, LLLG Faults	Minimal effect on energy and std_approx values.	Grid inverter control isolates DC bus from transient faults.
Load Switching	Very slight variations in std_approx and kurtosis.	DC microgrid adapts to step changes in demand.
Solar/WT Switching	Small changes in kurtosis, showing controlled system response.	Power converters manage generation transitions efficiently.

ISSN: 1311-1728 (printed version); ISSN: 1314-8060 (on-line version)

Islanding (80% SoC)	Higher std_approx but system remains stable.	Sufficient battery storage smooths DC voltage.
Islanding (20% SoC)	Significant drop in energy, increased std_approx and entropy.	Low SoC causes voltage instability due to reduced energy buffer.

Faults and renewable/load switching events have only transient impact, thanks to converter isolation and robust control systems. Islanding presents the most serious challenge, with stability wholly dependent on sufficient energy storage (battery SoC). DWT-based monitoring provides a reliable early warning indicator for the onset of instability and can be used to trigger pre-emptive control actions.

Practical recommendations: Enhance SoC monitoring, incorporate adaptive droop and virtual inertia controls, and consider hybrid storage strategies to fortify system stability during islanded operation

V. Conclusion

This study has demonstrated a Discrete Wavelet Transform (DWT)-based approach for transient stability assessment of hybrid AC–DC microgrids under faults, renewable/load switching, and islanding disturbances. The key findings are as follows:

- **Faults and switching events** result in short-lived deviations, with voltage dips (0.74–0.99 pu) and frequency variations (≤0.25 Hz) rapidly restored within 0.25 s due to inverter-based control and DC–AC decoupling.
- **Islanding with sufficient SoC (≥80%)** exhibits partial resilience but still shows noticeable instability, including voltage collapse to 0.15 pu and persistent oscillations.
- **Islanding with critically low SoC (20%)** leads to severe instability, with voltage collapse to 0.1 pu, sustained frequency deviations (49.75 Hz), and entropy escalation, indicating loss of dynamic coherence.
- **DWT-based statistical features** (energy reduction by ~50%, entropy and standard deviation rise during low SoC islanding) provide robust early indicators of instability not evident from raw waveforms alone.
- The analysis underscores that maintaining adequate SoC and employing advanced inverter controls (grid-forming, virtual inertia, adaptive droop) are critical to ensure stable islanded operation.

Future Work will focus on integrating the DWT-based monitoring framework with intelligent classifiers (ANN, SVM) for automated detection, hybrid energy storage management for enhanced islanding resilience, and hardware-in-the-loop (HIL) validation to translate simulation outcomes into practical deployment.

Volume 38 No. 9s, 2025
ISSN: 1311-1728 (printed version); ISSN: 1314-8060 (on-line version)

References

1. M. Jain et al., "Comprehensive review on control schemes and stability of microgrids," Energy Reports, 2023.
2. M. I. Abdelwanis et al., "A comprehensive review of hybrid AC/DC networks," Neural Comput. & Appl., 2024.
3. G. Meena et al., "Optimizing Power Flow and Stability in Hybrid AC/DC Grids," MDPI Energies, 2024.
4. S. Liaqat et al., "Transient stability enhancement in renewable microgrids," Int. J. Electr. Power Energy Syst., 2024.
5. H. Yang et al., "Adaptive Virtual Impedance Droop Control," IEEE Access, 2025.
6. Y. Xu et al., "Power quality issues in renewable-integrated distribution networks," IEEE Trans. Power Del., 2021.
7. IEEE PES, "Grid-Forming Inverter-Based Resource Research Landscape," 2024.
8. Q. Lin et al., "Inertia evaluations on grid-forming inverters," ECCE Conf., 2022.
9. Z. Zong et al., "Adaptive normalized droop control," IEEE Trans. Energy Convers., 2023.
10. S. C. Paiva et al., "Wavelet-based hybrid islanding detection," Renewable Energy, 2020.
11. I. Daubechies, Ten Lectures on Wavelets, SIAM, 1992.
12. S. Mallat, "A theory for multiresolution decomposition," IEEE TPAMI, 1989.
13. M. Uyar, "Effective wavelet-based feature extraction for PQ disturbances," EPSR, 2008.
14. Y. Wang et al., "Wavelet transform-based feature extraction for detection," IET Gener. Transm. Distrib., 2019.
15. V. Gogula et al., "Fault detection using db4 wavelet," Frontiers in Energy Research, 2023.
16. N. Giri et al., "Wavelet-based intelligent disturbance classification," Energies, 2024.
17. A. Cano et al., "DWT with neural networks for renewable microgrid faults," Int. J. Electr. Power Energy Syst., 2024.
18. Y. Huang et al., "Lifting-based wavelet for feature extraction," Signal Process., 2009.
19. C. Utrilla et al., "P/ω droop strategies for intermittent sources," IEEE Trans. Power Electron., 2024.
20. R. Georgious et al., "Review on energy storage in microgrids," Electronics, 2021.
21. A. Paspatis et al., "Advanced HIL testing for microgrids," Energies, 2024.
22. NREL, "HIL Test Bed for Microgrid Controller Testing," 2023.
23. E. Limpaecher et al., "Lessons learned from HIL testing," MIT Lincoln Lab, 2017.
24. M. Y. Worku et al., "Islanding detection methods for microgrids," Mathematics, 2021.
25. M. M. Islam et al., "Islanding detection and energy management in microgrids," Sustainability, 2021.
26. H. Liu et al., "Hybrid DWT-ANN for disturbance classification," IET Power Electron., 2022.

ISSN: 1311-1728 (printed version); ISSN: 1314-8060 (on-line version)

27. S. Kumar et al., "DWT-SVM for PQ disturbances," Int. J. Electr. Power Energy Syst., 2021.
28. Park et al., "Control of hybrid AC-DC microgrids," Renew. Sust. Energy Rev., 2022.
29. S. Islam et al., "Enhanced transient stability in hybrid microgrids," IET Renewables, 2025.
30. Chen et al., "Power quality in renewable networks," IEEE Trans. Power Del., 2021.
31. H. Yang et al., "Adaptive control in islanded microgrids," IEEE Access, 2025.
32. Z. Zong et al., "Normalized droop for stability," IEEE Trans. Energy Convers., 2023.
33. R. Georgious et al., "Hybrid storage for microgrids," Electronics, 2021.
34. H. Zhang et al., "Supercapacitor integration for DC stability," IEEE Trans. Smart Grid, 2023.
35. A. Paspatis et al., "Hardware-in-the-loop validation," Energies, 2024.
36. NREL, "Microgrid controller HIL framework," Tech. Rep., 2023.